

Evidence for multielectron resonances at the Sr *K* edge

P. D'Angelo* and H.-F. Nolting

EMBL Outstation Hamburg, c/o DESY, Notkestrasse 85, D-22603, Hamburg, Germany

N. V. Pavel

Dipartimento di Chimica, Università degli Studi di Roma "La Sapienza," Piazzale Aldo Moro 5, 00185 Roma, Italy

(Received 17 August 1995)

X-ray-absorption spectra of a Sr^{2+} aqueous solution have been studied in order to assess the contribution of double-electron excitation channels to the atomic background. Anomalies in the spectra have been identified that are assigned to the simultaneous excitation of $1s4s$, $1s3d$, and $1s3p$ electrons, referred to as KN_1 , $KM_{4,5}$, and $KM_{2,3}$ channels. A reliable determination of the double-electron edge parameters has been obtained by performing an analysis of the structural contribution in the correct framework of the radial distribution function theory. The experimental values of the energy onsets of the double-electron features are in excellent agreement with the predictions of the $Z+1$ approximation. The influence of double-electron effects on the determination of the structural parameters has been studied by using asymmetric peaks to model the Sr-O and Sr-H coordination shells. It has been found that an accurate determination of the structural parameters is possible only if double-electron channels are accounted for. The exclusion of these effects results in systematic errors on the structural parameters and, in particular, in a severe underestimation of the coordination numbers.

PACS number(s): 32.80.Fb, 32.30.Rj, 78.70.Dm, 87.64.Fb

I. INTRODUCTION

In the past several years an increasing amount of research work has been devoted to the study of multielectron transition processes in the x-ray-absorption spectra of different systems [1]. When an inner-shell vacancy is created by photoabsorption, electrons in the same atom have a small probability of being excited to an unoccupied state (shake-up) or ejected into the continuum (shake-off). Theoretical calculations have shown that, for noble gases, the shake-up probability has a sharp threshold onset while the shake-off probability increases linearly with photon energy [1–3]. This suggests that the multielectron excitation edges observed in x-ray-absorption spectra are mainly due to shake-up processes.

The absorption background of noble gases shows discrete resonances and slope changes that cannot be associated with the excitation of a single electron. Multielectron excitation features have been detected in the Ne [4], Xe [5], Ar [6], and Kr [7] absorption cross sections above the *K*-shell edge. Double-electron edges are also present in the spectra of bound atoms, but the oscillations due to the extended x-ray-absorption fine structure (EXAFS) prevent the immediate identification of such features. Nevertheless, the importance of accounting for double-excitation edges in the atomic background of condensed systems, in order to improve the EXAFS data analysis, has been pointed out by several groups [8–10].

The presence of the KN_1 , $KM_{4,5}$, and $KM_{2,3}$ edges has been observed above the Br *K* edge in the absorption spectra

of gaseous Br_2 , HBr [11], and brominated molecules [12]. The same features have been identified by Ito *et al.* [13] in the absorption spectra of Br^- in organic solvents. The *KM* transitions within the EXAFS oscillation have been recognized also in crystalline samples [10] and the *KL* double-electron edges have been widely studied in the absorption spectra of the third-period elements [9].

Strong *KN* and *KM* structures were found to affect the Rb *K* edge spectra of crystalline RbBr [10], bile acid rubidium salts, and Rb^+ aqueous solutions [14,15]. These features are similar to the double-electron channels of Kr, which is isoelectronic with Rb^+ . The aim of the present work is to study whether the multielectron excitation processes, which have been observed for Kr and Rb^+ , can be detected also for Sr^{2+} . Since the intensity of double-electron channels is usually only a few percent of the single-electron transition, their contribution to the absorption cross section in condensed systems is often masked by the single-electron EXAFS oscillations. Therefore we have decided to focus our attention on a Sr^{2+} aqueous solution where the EXAFS oscillations are expected to be weak. Recently, a method that uses molecular-dynamics (MD) pair distribution functions as relevant models in the calculation of the EXAFS structural signal has been employed in the study of the hydration shells of Br^- , brominated molecules [16], and Rb^+ [15]. This method allows a reliable calculation of the structural signal associated with the water molecules. By removing the EXAFS oscillation from the absorption spectrum it is possible to isolate the multielectron transition features and identify their positions. The solvation of strontium ion in water [17,18] and supercritical water [18] has been already investigated using the EXAFS technique. In both cases multielectron excitation processes have not been included in the atomic background. From the present analysis we have found that the inclusion of double-electron excitations plays a major role in

*Permanent address: Dipartimento di Chimica, Università degli Studi di Roma "La Sapienza," Piazzale Aldo Moro 5, 00185 Roma, Italy.

the correct determination of the structural parameters.

The paper is organized as follows. In Sec. II the experimental details will be presented. In Sec. III we discuss the evidence of the double-electron excitation channels in the absorption spectra. In Sec. IV the data analysis method is illustrated, and the results are presented in Sec. V.

II. EXPERIMENTAL SECTION

The EXAFS spectra above the strontium *K* edge of 0.1*M* and 3*M* SrCl₂ aqueous solutions have been recorded in the transmission mode using the EMBL spectrometer at HASYLAB [19]. Measurements were performed at room temperature using both a Si(220) and a Si(111) double-crystal monochromator [20]. For each spectrum an absolute energy calibration was performed [21]. Three spectra of each sample were recorded (50 min per spectrum) and averaged. The DORIS II storage ring was running at an energy of 4.45 GeV with electron currents between 70 and 40 mA. The solutions were kept in cells with a Teflon spacer and Kapton film windows. The thicknesses of the cell were 1 and 3 mm for the 3*M* and 0.1*M* samples, respectively. In the former case an optimum signal to noise ratio value was obtained (in the range 10⁴) with an absorption change over the edge of about one logarithmic unit, while in the latter the achieved edge jump was 0.5 logarithmic units. From the width of the peaks of the calibrator [21] the energy resolution of the Si(220) and Si(111) monochromator could be determined experimentally as 2.2 and 2.9 eV, respectively.

III. EXPERIMENTAL EVIDENCE OF THE MULTIELECTRON RESONANCE

Multielectron excitations in the x-ray-absorption cross section are associated with the presence of slope changes and anomalous structures in the atomic background. For condensed systems the identification of double-electron excitation features in the raw data is often hindered by the presence of the structural signal. An accurate characterization of the double-excitation edges affecting the Sr *K* edge could be obtained from a gas phase experiment. An alternative strategy, which is easier from an experimental point of view, is to choose a system where the amplitude of the structural contribution is low. For this reason we have performed measurements on an aqueous solution of Sr²⁺ at room temperature. Due to the small amplitude of the oxygen and hydrogen atoms and to the structural disorder, the EXAFS signal is weak and is confined to the low-energy region of the spectrum. Figure 1 shows the experimental data of the 3*M* SrCl₂ solution recorded with the Si(220) and Si(111) monochromator. Careful inspection of the magnified spectra shown in the lower part of the figure reveals the existence of two edgelike discontinuities in the absorption coefficient around 16 270 and 16 410 eV, which are similar to the *KM*_{4,5} and *KM*_{2,3} double-electron transitions observed for Rb⁺ [10,14,15]. Use of the Si(220) and Si(111) monochromators in the recording of the experimental data cleared any ambiguity that the features observed could be due to glitches produced by multiple reflections of the monochromator. The EXAFS spectrum of the 0.1*M* sample is identical to that of the 3*M* one, showing that the Sr²⁺ coordination, as well as the

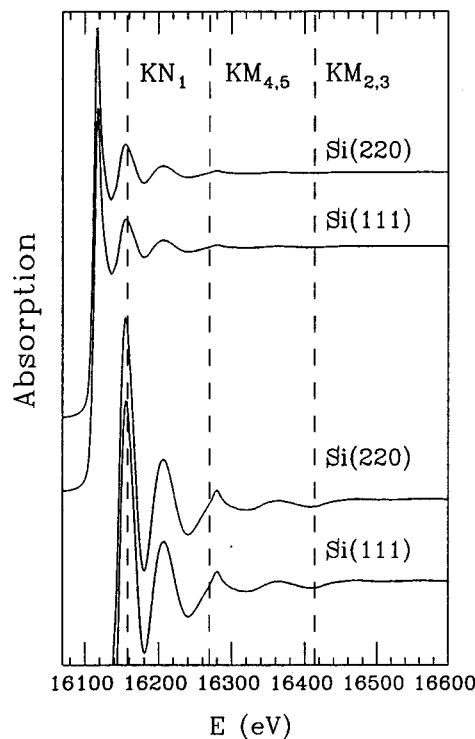


FIG. 1. X-ray-absorption spectra of Sr²⁺ in water near the *K* edge, recorded with a Si(220) and Si(111) monochromator. The spectra show the presence of slope changes (indicated by dashed lines) due to the 1*s*4*s*, 1*s*3*d*, and 1*s*3*p* double-electron excitations, namely, *KN*₁, *KM*_{4,5}, and *KM*_{2,3} edges, respectively. The lower curves are a magnification by a factor of 6.6 of the two above-reported spectra.

double-electron features, does not change for concentrations varying from 0.1*M* to 3*M*. The channel assignments in Fig. 1 have been obtained from the experimental data with the use of a proper background model as described in Sec. IV. The identification of the *KN*₁ edge in the raw data is hampered by the first EXAFS oscillation whose shape and amplitude is certainly affected by the presence of this double-electron transition.

The smooth polynomial spline, which is generally used to extract the structural oscillation, is not able to account for the discontinuities in the atomic background associated with double-excitation edges. It is well known that the residual part usually appears in the Fourier transform (FT) of the spectrum as a spurious peak at low distances [8,11,12]. The magnitude of the FT of the Si(220) EXAFS spectrum, extracted with a three segmented cubic spline function, is shown in Fig. 2. The FT has been obtained with a *k*³ weight in the interval *k* = 3.0–13.0 Å⁻¹ with no phase shift correction applied. Beside the structural peak at approximately 2.1 Å due to the water molecules, a further peak is observed around 0.9 Å, which cannot be assigned to any structural origin. Similar low-distance features have been observed in the FT spectra of several brominated compounds [11,12] and are associated with anomalies of the atomic background due to multielectron excitation effects.

IV. METHOD FOR DATA ANALYSIS

In order to fully characterize the multielectron transition features it is necessary to accurately determine the contribu-

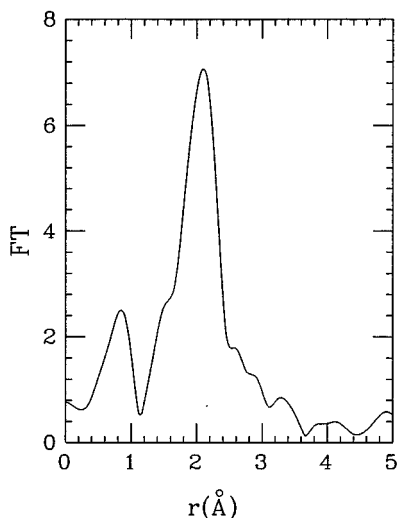


FIG. 2. Magnitude of the Fourier transform of the Sr^{2+} aqueous solution spectrum in the range $k=3.0\text{--}13.0 \text{ \AA}^{-1}$. The peak around 0.9 \AA has no structural meaning and is due to the double-electron excitation effects.

tion of the structural signal to the absorption cross section. For disordered systems the radial distribution function $g(r)$ around the photoabsorber atom is strongly asymmetric and the standard Gaussian approximation may produce significant errors even though an apparently reasonable fit to the data is obtained [22,23]. Recently, it has been shown that a deeper insight into the EXAFS data analysis can be provided by including additional external information on the radial distribution function obtained from MD simulations [16]. An accurate determination of the hydration shells of rubidium [15] and bromide ions, and brominated molecules [16], has been obtained from this method.

For disordered systems the $\chi(k)$ signal must be represented by the equation [24]

$$\chi(k) = \sum_j \int_0^\infty g_j(r) 4\pi r^2 \rho_j A_j(k, r) \sin[2kr + \phi_j(k, r)] dr, \quad (1)$$

where $g_j(r)$ is the radial distribution function associated with the j th species, $A_j(k, r)$ and $\phi_j(k, r)$ are the amplitude and phase functions, respectively, and ρ_j is the density of the scattering atoms. In spite of its high sensitivity to the short-range order, no information on the long-distance range can be obtained from the analysis of the $\chi(k)$ signal. This is due to the finite mean free path of the photoelectron $\lambda(k)$, which produces an exponential decay of the type $\exp[-r/\lambda(k)]$ and leads to an effective upper integration limit of $6\text{--}8 \text{ \AA}$ in Eq. (1). In our calculations, the photoelectron mean free path, as well as the additional damping factor accounting for the monochromator resolution, is included in the amplitude function $A_j(k, r)$ [16].

The theoretical signal associated with the water contribution has been calculated by means of Eq. (1) starting from the Sr-O and Sr-H pair distribution functions obtained by Spohr *et al.* [25] from MD simulations. The calculated $g(r)$'s refer to a $1.1m \text{ SrCl}_2$ aqueous solution at an average temperature of 298 K.

Phase shifts have been calculated in the muffin-tin approximation starting from overlapped spherically averaged relativistic atomic charge densities. One of the molecular distributions obtained from the MD simulations by Spohr *et al.* [25] has been used to calculate the phase shifts. The muffin-tin radii (R_{MT}) used were $1.59, 0.90,$ and 0.56 \AA for strontium, oxygen, and hydrogen atoms, respectively. It has been verified that changes in the R_{MT} values less than 10% do not produce detectable variations in the calculated signal. A Hedin-Lundqvist plasmon-pole approximation has been used for the self-energy part of the optical potential [26]. Inelastic losses of the photoelectron in the final state are accounted for intrinsically by complex potentials [27]. The imaginary part also includes a constant factor accounting for the known core-hole width ($\Gamma=3.25 \text{ eV}$) [28].

The theoretical signal $\chi(k)$ is related to the experimental absorption coefficient $\alpha(k)$ through the relation

$$\alpha(k) = \chi(k) J \sigma_0(k) + \beta(k) + J \sigma_0(k),$$

where $\sigma_0(k)$ is the atomic cross section, J is the edge jump, and $\beta(k)$ is the background function, which accounts for further absorbing processes. Double-electron excitations are accounted for by modeling the $\beta(k)$ function as the sum of a smooth polynomial spline plus step-shaped functions as already described for the Br K edge [12]. This model background is then summed to the structural contribution to build a theoretical model signal that is fitted to the raw data. Each double-electron channel depends on three parameters representing the edge position E_d , the width DE , and the relative jump H . A good estimation of the shake-up channel onset energy can be obtained from the $Z+1$ approximation while an empirical determination of the shape and the intensity of the double-excitation features can be provided from the H and DE values obtained from the fitting procedure.

In the standard EXAFS data analysis the theoretical signal depends on several parameters that are refined in order to achieve the best fit to the experimental data. In our case an estimate of $g_j(r)$ has been obtained from MD simulations [25] and the only nonstructural parameters related to the $\chi(k)$ signal that have been minimized are E_0 and S_0^2 . E_0 is the photon energy required for the transition to the continuum threshold and allows the theoretical and the experimental energy scales to be compared. S_0^2 provides a uniform reduction of the signal and is associated with many-body effects. As previously shown, this parameter is expected to be equal to one when multielectron-excitation effects are properly included in the atomic background [11,12]. The remainder of the nonstructural parameters, namely, the photoelectron damping and the core-hole lifetime, have been included directly in the theory. A fixed experimental value of the monochromator resolution, obtained from the calibration procedure [21], was used during the minimization.

V. RESULTS AND DISCUSSION

The first step of the data analysis involved the calculation of the theoretical signal by means of Eq. (1), starting from the Sr-O and Sr-H pair distribution functions obtained from the MD simulations. With our approach a reliable estimate of the structural contribution to the absorption cross section is

TABLE I. Double-electron excitation edge parameters obtained from the fitting procedure and comparison with the $Z+1$ predictions. The double-excitation energy onset E_d is measured from the K edge threshold energy (E_t). The absorption discontinuities H are given in K edge jump units and the energies and the width parameter DE are given in eV.

Excitation	$E_d - E_t$	H	DE	E_{Z+1}
KN_1	45	0.133	21	43.8
$KM_{4,5}$	156	0.011 3	45	155.8–157.7
$KM_{2,3}$	301	0.002 86	70	298.8–310.6

employed. This allows the background parameters to be fitted and correctly determined. The validity of the starting $g(r)$ models can be assessed by the agreement of the experimental and theoretical data. Least-squares fits of the experimental data collected with the Si(220) monochromator have been performed in the range $k = 3.0\text{--}15.2 \text{ \AA}^{-1}$ using the FITHEO computer program [29]. The fit index R_i is defined by Eq. (5) of Ref. [12] and a weighting value of 2.5 has been applied. From the minimization procedure it has been found that the best fit of the calculated signal to the experimental data is obtained when the average distances of the Sr-O and Sr-H MD radial distribution functions are decreased by 0.06 and 0.04 \AA , respectively. In addition, the zero position of the theoretical energy scale was found at 0.5 ± 0.2 eV above the first inflection point of the spectrum and S_0^2 was found to be equal to one. Three step-shaped functions have been included in the atomic background to account for the $1s4s$, $1s3d$, and $1s3p$ double-electron excitation edges (namely, KN_1 , $KM_{4,5}$, and $KM_{2,3}$). In Table I we report the experimental energy differences between the double-electron channel onsets (E_d) and the K edge threshold (E_t), together with the H and DE values obtained from the minimization. The threshold energy E_t is defined by the first inflection point of the absorption spectrum. The energies are measured in eV and the intensity is measured in K edge jump units. The positions of the double-electron features are in excellent agreement with the predictions of the $Z+1$ approximation as listed in Table I. Note that the j energy splitting of the $3d_{5/2}$ and $3d_{3/2}$ and of the $3p_{3/2}$ and $3p_{1/2}$ electrons obtained from the $Z+1$ approximation is too small to be resolved. Total-energy Dirac-Fock calculations have been performed by Filipponi and Di Cicco [30] for all fifth-period elements. Theoretical values of the onset energies for the $KM_{4,5}$ and $KM_{2,3}$ Sr double-excitation edges have been estimated by means of total-energy differences and they are in good agreement with the experimental values reported in Table I. The H parameter accounts for the intensity of the double-excitation edges; the experimental values of the shake-up probabilities are found to increase for the outer shells and to become quite large for the KN_1 edge. The same trend has been found previously both from theoretical [31] and experimental investigations [32].

As already observed for Rb [14,15], the $KM_{4,5}$ channel presents a sharp feature that still remains in the structural signal as a nonstructural peak at about 6.6 \AA^{-1} after background subtraction. In order to perform a reliable determination of the structural parameters the experimental points in a range of about 20 eV around this peak have been excluded

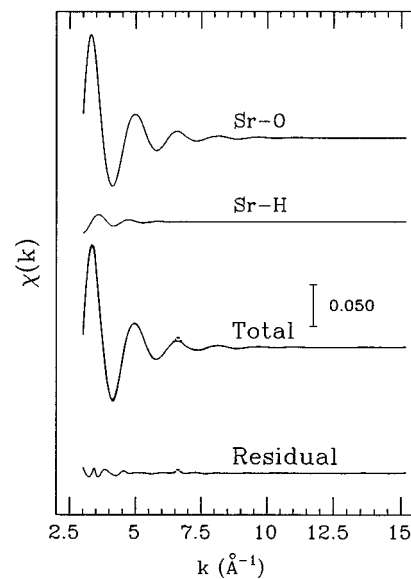


FIG. 3. Fit of the Sr^{2+} aqueous solution spectrum. From top to bottom the following curves are reported: Sr-O and Sr-H theoretical signals calculated on the basis of the MD $g(r)$'s and the sum of the previous contributions compared with the experimental spectrum and residual.

from the fitting procedure. It is important to stress that the slope change associated with the opening of this channel is correctly reproduced by the model background since the resulting $\chi(k)$ signal is a damped sine wave, which one would expect for a simply coordinated disordered system (see Fig. 3). Distortions in the EXAFS spectrum of a similar system have been detected by Persson *et al.* [17] with a standard background subtraction and the anomalies in the amplitude hampered a reliable determination of the coordination numbers.

The results of the fitting procedure applied to the $3M$ spectrum are shown in Fig. 3. The first two curves from the top correspond to the Sr-O and Sr-H signal calculated from the MD $g(r)$'s. The lower part of the figure shows the total theoretical contribution compared with the experimental spectrum and the resulting residual. The agreement between the experimental and the theoretical signal is excellent and a $R_i = 0.110 \times 10^{-6}$ has been obtained. From Fig. 3 it is evident that the total signal is dominated by the Sr-O contribution, while the Sr-H signal is weaker and mainly affects the low- k region of the spectrum. However, the inclusion of this contribution has been found to be essential to properly reproduce the experimental spectrum in the low- k region. The accuracy of the data analysis can be appreciated by looking at the magnitude of the FT of the experimental, theoretical, and residual curves of Fig. 3 (see Fig. 4). The spurious low distance peak is no longer present and the excellent agreement between theory and experiment is possible only with the inclusion of the double-excitation contribution.

We also performed an analysis of the EXAFS spectrum using a conventional three-region polynomial spline to model the atomic background. The results are shown in Fig. 5. The agreement between the theoretical and the experimental signals is not satisfactory ($R_i = 0.325 \times 10^{-5}$), especially in the low- k region and the residual curve shows a pattern

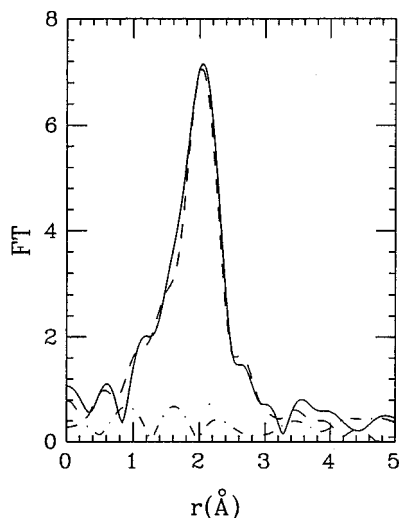


FIG. 4. Fourier transforms of the Sr^{2+} aqueous solution experimental spectrum compared with the total theoretical signal calculated from the MD $g(r)$'s and residual. The $\chi(k)$ experimental signal has been obtained by subtracting an atomic background that includes the double-electron excitation edges. The FT's have been calculated in the range $k = 3.0\text{--}13.0 \text{ \AA}^{-1}$.

with a marked cusp at 3.4 \AA^{-1} and two step-shaped thresholds around 6.4 and 8.9 \AA^{-1} . The energy positions of these three features (indicated in Fig. 5 by arrows), correspond to the onset energies of the KN_1 , $KM_{4,5}$, and $KM_{2,3}$ edges, respectively. The shape of the $KM_{4,5}$ edge, shown in the magnified section of the spectrum of Fig. 5, is reminiscent of the K absorption threshold. A white line feature, followed by

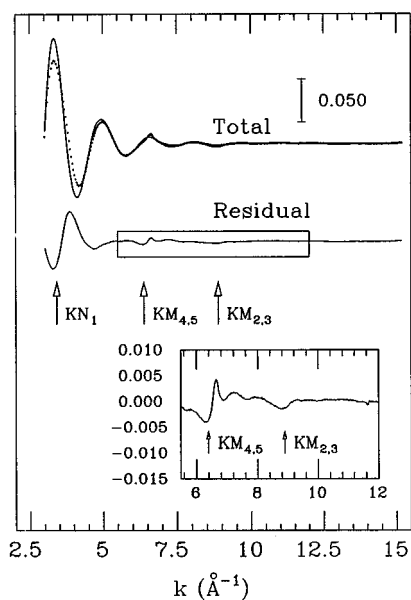


FIG. 5. Comparison of the total theoretical curve calculated from the MD $g(r)$'s (solid line) with the $\chi(k)$ experimental spectrum (dots) extracted without the inclusion of the double-excitation edges. The residual curve shows the presence of three well-defined steps at about 3.4 , 6.4 , and 8.9 \AA^{-1} , which are associated with the KN_1 , $KM_{4,5}$, and $KM_{2,3}$ double-excitation edges.

an oscillating signal, is clearly detectable. The similarity of the oscillation frequency above the $KM_{4,5}$ channel to that of the Sr-O structural signal suggests that these features could be due to an EXAFS effect over the double-excitation edge. Due to the approximation in the theory, the calculated structural signal is less reliable in the low- k region and the identification of this effect at the KN_1 edge is less straightforward. In the case of the $KM_{2,3}$ edge, the intensity of the channel is too low to detect any feature above the threshold. A more detailed investigation is necessary to allow the conclusive explanation of this phenomenon. As already observed, the intensity of the KN_1 channel is high, causing the amplitude and the frequency of the $\chi(k)$ first oscillation to be seriously distorted. As a consequence, the structural results obtained from a standard data analysis are expected to be affected by systematic errors, especially if the low- k region of the spectrum is included.

Further progress in the understanding of the effect of the multielectron excitations on the structural signal has been obtained by applying a peak fitting procedure that refines the short-range shape of the MD $g(r)$. In the case of disordered systems the radial distribution function around the photoabsorber atom is asymmetric and incorrect structural parameters will be obtained if the EXAFS spectrum is analyzed using the standard Gaussian approximation [22,23,33,34]. Recently, it has been shown that proper starting models can be obtained by decomposing the MD $g(r)$ into an asymmetric peak and a long-distance tail [16]. The tail contribution is usually calculated by means of Eq. (1), and due to the small sensitivity of the $\chi(k)$ signal to the long distance range, it is kept fixed during the minimization. In our case both the Sr-O and Sr-H tail signals have been found to be negligible and therefore they have not been considered. As described elsewhere [16], the asymmetric peaks are modeled with a gamma-like distribution function that depends on four parameters: the coordination number N , the average distance R , the distance mean-square variation σ^2 , and the skewness β . Due to the asymmetry, the average distance R does not coincide with the modal value of the distribution. This model function is very flexible and can be used both for peaks with small and large asymmetry.

The $\chi(k)$ signals associated with the asymmetric peaks have been calculated by means of the GNXAS program [29] and a fitting procedure has been applied to the peak parameters in order to obtain the best fit between the theoretical and the experimental spectrum. The fitting allowed us to probe and refine the short-range shape of the Sr-O MD $g(r)$. The best-fit analysis of the $3M$ spectrum, performed in the range $k = 3.0\text{--}15.2 \text{ \AA}^{-1}$, is reported in Fig. 6. The first two curves at the top of the figure correspond to the Sr-O and Sr-H theoretical signals calculated from the refined asymmetric peaks. The remainder of the figure shows the total theoretical contribution compared with the experimental spectrum and the resulting residual. The peak parameters obtained from the fitting procedure are listed in Table II and the values of E_0 and S_0^2 are equal to those obtained from the previous analysis. After the minimization the structural parameters have been found to differ from the MD starting values; in particular, the Sr-O and Sr-H first peaks were found to be shifted to shorter distances by 0.08 and 0.02 \AA , respectively. This result is in agreement with the shift of the

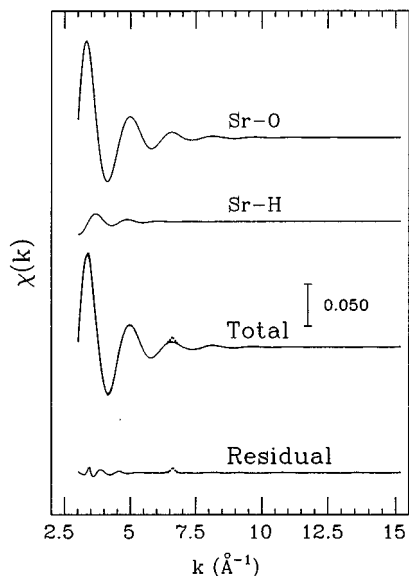


FIG. 6. Fit of the Sr^{2+} aqueous solution spectrum. From top to bottom the following curves are reported: Sr-O and Sr-H theoretical signals calculated by means of asymmetric peaks and the sum of the previous contributions compared with the experimental spectrum and residual.

MD $g(r)$'s observed from the previous analysis. A difference of less than 2% has been observed for the other parameters with the exception of the variance and the skewness of the Sr-H pair distribution function, which were 13% larger and 5% smaller than the initial values, respectively. Better agreement between the experimental and the calculated curves has been obtained with respect to the previous analysis and this result is confirmed by the fit index value ($R_i = 0.915 \times 10^{-7}$). The refined values of the double-excitation channel onsets have been found to be equal to those in Table I. A difference of less than 3% has been obtained for the H and DE parameters. The same procedure has been applied to the 0.1M spectrum and all the refined parameters were found within the errors reported in Table I.

The statistical significance of the present least-squares fitting procedure should be noted. According to well-established criteria [35], a rough estimate of the number of parameters that can be refined is given by the $2\Delta k\Delta r/\pi + 2$ relation, which supports the present least-squares fitting procedure. Δk is the k space over which the $\chi(k)$ signal is fitted and Δr is the width of the r -space Fourier filter window. In our case Δk is approximately 12 \AA^{-1} and Δr is limited by the mean-free path only, as we are not Fourier filtering the data.

At this point the problem of the accuracy of the structural

parameters listed in Table II needs to be addressed. As already shown [34], standard statistical concepts [36] can be used to estimate the errors affecting the fitted values of the parameters, since the data analysis is performed using the raw spectrum. Statistical standard deviations and correlation effects have been evaluated by using correlation maps for each couple of parameters. Standard deviation have been obtained from confidence region ellipses containing 68.3% of normally distributed data, as described elsewhere [34]. A positive correlation has been found between E_0 and R_O , σ_O^2 and N_O , R_O and σ_O^2 , and R_O and β_O , while there is no correlation between all the other possible couples of structural parameters associated with the Sr-O shell. The existence of a correlation between E_0 and the shell distance and between the Debye-Waller factor and the coordination number is a well-known phenomenon in the EXAFS data analysis performed in the Gaussian approximation. Due to the analytical function used to describe the asymmetric peak, σ_O^2 and β_O are also correlated to R_O in this case, as R is the average distance and not the modal value of the distribution and the full width at half maximum peak is defined both by β and σ . The errors affecting the first peak parameters are very small and an accurate determination of the Sr-O coordination number has been obtained. A different result has been found for the Sr-H shell. In this case a strong positive correlation between σ_H^2 and N_H and between R_H and β_H has been observed. This effect is responsible for the large uncertainty of the Sr-H coordination number and, in general, for the larger errors associated with the Sr-H shell fitted parameters.

The two asymmetric peaks obtained from the iteration procedure are compared with the MD $g(r)$ models in Fig. 7. A different position of the first rise of the Sr-O $g(r)$ can be clearly seen. A shift of the $g(r)$ first peak towards shorter distances, with respect to the MD model, has been already observed in other cases [16]. These results suggest that the EXAFS technique can be employed to check and improve the potential-energy functions and partial charges used in the MD simulations. The strong short-range sensitivity of the EXAFS technique allowed a very accurate determination of the short-range properties of the Sr-O $g(r)$, whereas the accuracy of the long-distance tail relies completely on the original model. In the case of the Sr-H radial distribution function, satisfactory agreement between the refined asymmetric peak and the MD starting model has been observed, which demonstrates the validity of the data analysis performed with the inclusion of the hydrogen contribution. However, the low accuracy of the refined parameters does not allow a refinement of the short-distance shape of the MD $g(r)$ on the basis of the EXAFS information. The presence of the hydrogen contribution in the first coordination shell

TABLE II. Structural parameters of the Sr-O and Sr-H asymmetric peaks obtained from the EXAFS analysis: R represents the average distance, σ^2 represents the vibrational variance, β is the asymmetry parameter, and N is the coordination number. The standard deviations are given in parentheses.

Peak	R (Å)	σ^2 (Å ²)	β	N
Sr-O	2.643 (0.002)	0.021 (0.002)	0.61 (0.01)	10.3 (0.1)
Sr-H	3.40 (0.02)	0.05 (0.01)	0.27 (0.15)	22 (9)

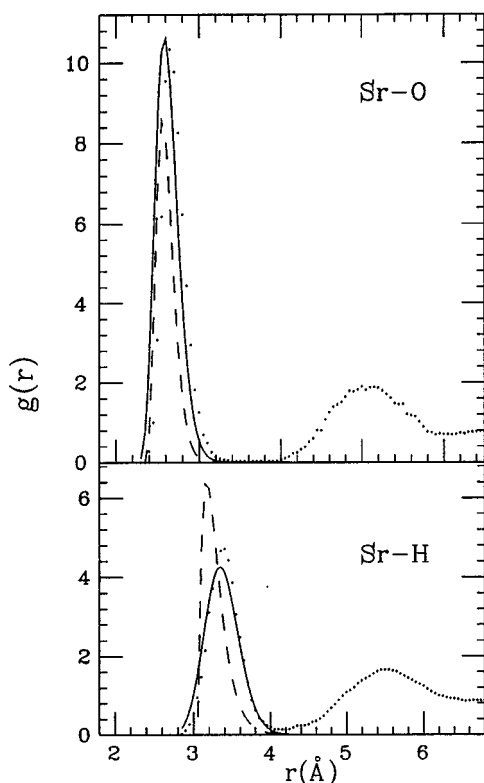


FIG. 7. From top to bottom: Sr-O and Sr-H asymmetric peaks obtained from the EXAFS analysis performed with the inclusion (solid line) and the exclusion (dashed line) of the double-excitation edges, compared with the $g(r)$'s obtained by Sphor *et al.* [25] from the MD simulations.

was recently individuated in the EXAFS spectrum of bromide ion in methanol [34].

Finally, it would be of interest to observe the effect of the omission of the double-excitation contributions on the refined values of the structural parameters. A fitting procedure has been applied to the EXAFS spectrum extracted with a conventional smooth spline function as previously described. The refined parameters obtained from the minimization are $R_O = 2.62 \text{ \AA}$, $\sigma_O^2 = 0.013 \text{ \AA}^2$, $\beta_O = 0.79$, and $N_O = 6.3$ for the first shell and $R_H = 3.30 \text{ \AA}$, $\sigma_H^2 = 0.03 \text{ \AA}^2$, $\beta_H = 1.41$, and $N_H = 18$ for the second shell. The fit index is 0.214×10^{-6} and, due to the omission of the double-electron contribution, a value of 0.8 has been found for S_0^2 . By comparing these values with those of Table II, it appears that the coordination numbers are severely underestimated when double-excitation effects are not included and also the other parameters are perturbed. The overall effect on the position and shape of the asymmetric peaks is clearly visible in Fig. 7, where the refined shells are compared with those obtained from the previous analysis performed with the inclusion of the double-electron edges. This result is consistent with that of Persson *et al.* [17], even though they performed the data analysis in the Gaussian approximation, without minimizing the coordination numbers. Pfund, Darab, and Fulton [18] performed an EXAFS analysis of a 0.2M Sr^{2+} aqueous solution only in an extremely limited range of the spectrum ($k = 2.0\text{--}5.8 \text{ \AA}^{-1}$). By applying the ratio method a Sr-O first-neighbor

distance of 2.62 \AA and a coordination number of 7.3 have been obtained. The short energy range of the spectrum used in the analysis does not include the $KM_{4,5}$ and $KM_{2,3}$ double-excitation edges, but an inaccuracy on the structural parameter is expected from the inclusion of the KN_1 edge. Also in this case a nonstructural peak at about 1.1 \AA is detectable in the FT of the experimental spectrum. X-ray diffraction measurements performed by Albright [37] and by Caminiti *et al.* [38] on SrCl_2 aqueous solutions have led to Sr-O first shell distances of 2.67 and 2.64 \AA , respectively. A Sr-O coordination number of 7.8 has been obtained by Albright and the value of 8 reported by Caminiti *et al.* has been determined by a model fit. These results reflect the difficulty of the x-ray-diffraction (XRD) technique to determine a reliable value of hydration numbers and enforces the EXAFS technique as a valid tool in the structural investigation of disordered systems. The EXAFS technique is more selective than x-ray neutron diffraction, since the partial distribution functions corresponding to a single atomic type can be determined. For an N -component system the $g(r)$ extracted from the x-ray-absorption spectroscopy signal contains the overlap of N independent pair distribution functions, whereas the XRD experiments give the contribution of all interatomic distances in the sample. In the case of aqueous salt solutions, a severe overlap between the metal ion-solvent and the solvent-solvent distances is present in the XRD data. Therefore, reliable results on the hydration structure around the metal ions could be only achieved by applying a difference procedure to eliminate the bulk water contribution. Moreover, with the EXAFS technique, overlapped $g(r)$'s are better resolved since the EXAFS oscillations are clearly detectable up to $k \cong 10 \text{ \AA}^{-1}$, which corresponds to about $k = 20 \text{ \AA}^{-2}$ in the diffraction scale. From this study it is evident that, if a thorough analysis is carried out, the EXAFS technique can provide valuable short-distance structural information on disordered systems, which is not possible with other experimental techniques.

VI. CONCLUSION

A detailed investigation of the x-ray-absorption spectrum of a Sr^{2+} aqueous solution has been performed. The existence of double-excitation channels at the Sr K edge has been clearly shown. The contribution of the KN_1 , $KM_{4,5}$, and $KM_{2,3}$ double-electron excitation channels has been studied by analyzing the EXAFS spectrum in the correct framework of the radial distribution function theory. The Sr-O and Sr-H signals have been calculated starting from realistic $g(r)$ models obtained from MD simulations. A proper background model has been used to derive the double-excitation edge parameters. The experimental values of the energy onset of the multielectron transitions are in excellent agreement with the prediction of the $Z+1$ approximation. From this analysis it is clear that the inclusion of these additional channels is essential to obtain good agreement between the experimental and the theoretical data.

A deeper insight into the influence of the double-electron effects on the correct determination the structural parameters has been obtained by using asymmetric peaks to model the Sr-O and Sr-H coordination shells. The initial asymmetric peaks were derived from the MD $g(r)$'s and the use of a

fitting procedure allowed an accurate determination of the structural parameters. A method based on well-established statistical concepts has been used to calculate statistical errors of the fitting values.

This study demonstrates that a reliable determination of the structural parameters is possible only if the double-excitation edges are accounted for. The exclusion of these effects results in systematic errors on the structural parameters and in particular in a severe underestimation of the coordination numbers. The shape and the energy onsets of the double-excitation edges are expected to change according to the chemical environment of the absorbing atom. However, the results of the present investigation provide an invaluable insight and guideline for the correct analysis of any

x-ray-absorption spectrum at the Sr K edge and in general in any spectrum where multielectron resonances are present.

ACKNOWLEDGMENTS

The authors gratefully acknowledge Dr. Eckhard Spohr for providing one of the configurations of the MD simulations. We thank the European Union for support of the work at EMBL Hamburg through the HCMP Access to Large Installation Project, Contract No. CHGE-CT93-0040. P.D'A. was supported by EU Contract No. ERBCHBGCT930485. This work was sponsored by the Italian Consiglio Nazionale delle Ricerche and by the Italian Ministero per l'Università e per la Ricerca Scientifica e Tecnologica.

-
- [1] S. J. Schaphorst, A. F. Kodre, J. Ruschinski, B. Crasemann, T. Åberg, J. Tulkki, M. H. Chen, Y. Azuma, and G. S. Brown, *Phys. Rev. A* **47**, 1953 (1993), and references therein.
- [2] G. B. Armen, T. Åberg, K. Karim, J. Levin, B. Crasemann, G. Brown, M. Chen, and G. Ice, *Phys. Rev. Lett.* **54**, 182 (1985).
- [3] Y. Ito, H. Nakamatsu, T. Mukoyama, K. Omote, S. Yoshikado, M. Takashi, and S. Emura, *Phys. Rev. A* **46**, 6083 (1992).
- [4] J. M. Esteva, B. Gauthé, P. Dhez, and C. R. Karnatak, *J. Phys. B* **16**, L263 (1983).
- [5] M. Deusch and P. Kizler, *Phys. Rev. A* **45**, 2122 (1992).
- [6] R. D. Deslattes, R. E. LaVilla, P. L. Cowan, and A. Henins, *Phys. Rev. A* **27**, 923 (1983).
- [7] E. Bernieri and E. Burattini, *Phys. Rev. A* **35**, 3322 (1987).
- [8] A. Filipponi, E. Bernieri, and S. Mobilio, *Phys. Rev. B* **38**, 3298 (1988).
- [9] A. Filipponi, T. A. Tyson, K. O. Hodgson, and S. Mobilio, *Phys. Rev. A* **48**, 1328 (1993).
- [10] G. Li, F. Bridges, and G. S. Brown, *Phys. Rev. Lett.* **68**, 1609 (1992).
- [11] P. D'Angelo, A. Di Cicco, A. Filipponi, and N. V. Pavel, *Phys. Rev. A* **47**, 2055 (1993).
- [12] E. Burattini, P. D'Angelo, A. Di Cicco, A. Filipponi, and N. V. Pavel, *J. Phys. Chem.* **97**, 5486 (1993).
- [13] Y. Ito, T. Mukoyama, S. Emura, M. Takahashi, S. Yoshikado, and K. Omote, *Phys. Rev. A* **51**, 303 (1995).
- [14] E. Giglio, S. Loreti, and N. V. Pavel, *J. Phys. Chem.* **92**, 2858 (1988).
- [15] P. D'Angelo, A. Di Nola, E. Giglio, M. Mangoni, and N. V. Pavel, *J. Phys. Chem.* **92**, 2858 (1995).
- [16] P. D'Angelo, A. Di Nola, A. Filipponi, N. V. Pavel, and D. Roccatano, *J. Chem. Phys.* **100**, 985 (1994).
- [17] I. Persson, M. Sandström, H. Yokoyama, and M. Chaudhry, *Z. Naturforsch. Teil A* **50**, 21 (1995).
- [18] D. M. Pfund, J. G. Darab, and J. L. Fulton, *J. Phys. Chem.* **98**, 13 102 (1994).
- [19] C. Hermes, E. Gilbreg, and M. H. J. Koch, *Nucl. Instrum. Methods* **222**, 207 (1984).
- [20] R. F. Pettifer and C. Hermes, *J. Phys. (Paris) Colloq.* **47**, C8-127 (1986).
- [21] R. F. Pettifer and C. Hermes, *J. Appl. Cryst.* **18**, 404 (1985).
- [22] P. Eisenberger and G. S. Brown, *Solid State Commun.* **29**, 481 (1979).
- [23] E. D. Crozier and A. J. Seary, *Can. J. Phys.* **58**, 1388 (1980).
- [24] E. D. Crozier, J. J. Rehr, and R. Ingalls, in *X-Ray Absorption: Principles, Applications, Techniques of EXAFS, SEXAFS, and XANES*, edited by D. C. Koningsberger and R. Prins (Wiley, New York, 1988), Chap. 9.
- [25] E. Spohr, G. Pálincás, K. Heinzinger, P. Bopp, and M. M. Probst, *J. Phys. Chem.* **92**, 6754 (1988).
- [26] L. Hedin and B. I. Lundqvist, *J. Phys. C* **4**, 2064 (1971).
- [27] S.-H. Chou, J. J. Rehr, E. A. Stern, and E. R. Davidson, *Phys. Rev. B* **35**, 2604 (1987); T. A. Tyson, M. Benfatto, C. R. Natoli, B. Hedman, and K. O. Hodgson, *Physica B* **158**, 425 (1989); T. A. Tyson, K. O. Hodgson, C. R. Natoli, and M. Benfatto, *Phys. Rev. B* **46**, 5997 (1992).
- [28] M. O. Krause and J. H. Oliver, *J. Phys. Chem. Ref. Data* **8**, 329 (1979).
- [29] A. Filipponi, A. Di Cicco, T. A. Tyson, and C. R. Natoli, *Solid State Commun.* **78**, 265 (1991); A. Filipponi and A. Di Cicco, *Synchrotron Radiat. News* **6**, 13 (1993); T. E. Westre, A. Di Cicco, A. Filipponi, C. R. Natoli, B. Hedman, E. I. Solomon, and K. O. Hodgson, *J. Am. Chem. Soc.* **117**, 1566 (1995).
- [30] A. Filipponi and A. Di Cicco, *Phys. Rev. A* **52**, 1072 (1995).
- [31] T. Mukoyama and Y. Ito, *Bull. Inst. Chem. Res. Kyoto Univ.* **71**, 398 (1994).
- [32] A. Filipponi and A. Di Cicco, *Phys. Rev. B* **51**, 12 322 (1995).
- [33] E. D. Crozier, *Physica B* **208**, 330 (1995).
- [34] P. D'Angelo, A. Di Nola, M. Mangoni, and N. V. Pavel, *J. Chem. Phys.* (to be published).
- [35] Report of the International Workshop on Standards and Criteria in X-Ray Absorption Spectroscopy, *Physica B* **158**, 701 (1989); E. A. Stern, *Phys. Rev. B* **48**, 9825 (1993).
- [36] W. H. Press, S. A. Teukolsky, W. T. Vetterling, and B. P. Flannery, *Numerical Recipes* (Cambridge University Press, Cambridge, 1992), Chap. 15.6, p. 689.
- [37] J. N. Albright, *J. Chem. Phys.* **56**, 3783 (1972).
- [38] R. Caminiti, A. Musinu, G. Paschina, and G. Pinna, *J. Appl. Crystallogr.* **15**, 482 (1982).